
Research on Electro-Mechanical Brake Systems Control Method for Mine Underground Electric Trackless Rubber-Tired Vehicle

[Jian Li](#) , [Xingmin Xiao](#) , [Zhong kai Li](#) , [Chi Ma](#) *

Posted Date: 24 August 2023

doi: 10.20944/preprints202308.1735.v1

Keywords: Mine electric trackless rubber-tired vehicle; Brake-by-wire; Electro-Mechanical Brake actuator; Active braking system; Force/Position switch strategy



Preprints.org is a free multidiscipline platform providing preprint service that is dedicated to making early versions of research outputs permanently available and citable. Preprints posted at Preprints.org appear in Web of Science, Crossref, Google Scholar, Scilit, Europe PMC.

Copyright: This is an open access article distributed under the Creative Commons Attribution License which permits unrestricted use, distribution, and reproduction in any medium, provided the original work is properly cited.

Article

Research on Electro-Mechanical Brake Systems Control Method for Mine Underground Electric Trackless Rubber-Tired Vehicle

Jian Li ¹, Xingming Xiao ², Zhongkai Li ³ and Chi Ma ^{*}

¹ School of Mechatronic Engineering, China University of Mining and Technology, Xuzhou 221116, China; lijian0609SEU@163.com

² School of Mechatronic Engineering, China University of Mining and Technology, Xuzhou 221116, China; xxm_cumt@163.com

³ School of Mechatronic Engineering, China University of Mining and Technology, Xuzhou 221116, China; machicumt@163.com

* Correspondence: machicumt@163.com; Tel:13775985809

Abstract: Electro-mechanical braking(EMB) which represents development direction of autonomous and intelligent braking plays very useful role on enhancing the braking response performance and intelligence level for mine underground electric trackless rubber-tired vehicle (ETRV). However, there is no Electro-Mechanical Brake system applied practically in coal mine UTRV until now. The accurate control of braking clamping force can determine the length and precision of braking distance of mine ETRV. In addition, because of poor working conditions in underground coal mine tunnel, braking clamping force sensor may be easy to occur failure, which may cause vital accident. Therefore, a cascaded three-closed-loop EMB system with a positive clamping force sensor or force estimator built for ETRV is established to achieve autonomous elimination and reset of braking clearance and reliable braking force tracking ability via utilizing the electro motor rotor angle displacement and hysteresis effect of mechanical components in this EMB. The results of simulation and experiment indicate that clamping force response is faster than traditional hydraulic disk braking system and proposed force estimator presents good fault-tolerant ability when sensor is fault. This EMB can replace the current hydraulic brake system to enhance automation level of braking control for ETRVs and braking force response performance, reduce oil pollution and cost of maintenance, which is also key technology support for really precise motion control of mine autonomous driving vehicles.

Keywords: mine electric trackless rubber-tired vehicle; brake-by-wire; electro-mechanical brake actuator; active braking system; force/position switch strategy

1. Introduction

In a longer period from now, coal resources must keep accounting for majority of energy consumption in China and continue to be widely used in all over the world¹. Underground electric trackless rubber-tired vehicle(ETRV) is an efficient and green auxiliary transportation vehicle in the underground coal mine production, which takes task of transporting persons or materials between surface and underground and can transfer mining machinery and materials from one working area to another new area obviously faster than other existing transportation tools. The existing braking system of mine ETRV generally uses disk braking structure, which consists of braking pedal, hydraulic pressure pins, piston, braking caliper and braking pads², where braking torque is generated by friction force between braking pads and disk, which further derived from pressure of highly compressed hydraulic oil. Although traditional hydraulic disc brakes are applied currently, there are some obvious disadvantages such as more complex structure, slower response under low

environmental temperature, larger components account, potential pollution risk of oil leak, lower automation level³. And this traditional one is impossible to be integrated into intelligent chassis control system of automated mine vehicle. Therefore, it's significantly valuable to consider adopting a novel brake-by-wire system with pure mechanical transmission structure controlled by high-performance micro controller unit (MCU). Aiming to ensure safety of drivers, materials, vehicle-self and concerning traffic participants and achieve reliable braking performance of autonomous driving for intelligent mine, it is very necessary to research accurate and reliable EMB actuator and its control method for UTRVs in coal mine.

However, related scholars also still stay on stage of theoretical research or experimental prototype test, meanwhile there is no any mature braking system product sold on market so far. Especially, there is no practical engineering application of EMB device in both ETRV and other type of transportation vehicles in coal mine, which restrict development of underground unmanned transportation system.

Fortunately, there are some research achievements of EMB system in passenger cars published in journals and other documents in most recent years. Jin and Feng et al.⁴ built a EMB bench and test both the open-loop control method and single force close-loop control method on it. Dealing with improving tracking control ability of the braking force, He Cheng et al.⁵ designed the braking torque closed-loop control based on switch-reluctance-motor, in which estimated value of braking torque only lags behind the actually measured value of torque sensor by just one electrical period and it can achieve fast close-loop regulator. Xiao and Gong et al.⁶ have used a linear motor to design a novel brake-by-wire actuator, which can omit motion conversion mechanism and provides a new design idea for BBW actuator. For solving nonlinear and disturbance problems of EMB system, Soohyeon Kwon et al.⁷ consider EMB to be affected by both linear part and nonlinear one, and further design a force status estimator based on Kalman filter. Zhao et al.⁸ proposed a slide-mode reaching law to deal with load torque variation. Focusing on friction and gap distance detection, Chihoon Jo et al.⁹ established a friction model which involves friction effect of the motor and mechanical motion parts, and then utilized motor torque gradient change to achieve initial gap distance control. In field of mine auxiliary transportation, Jin et al.¹⁰ combine PI and Linear quadratic regulator (LQR) to control positive pressure of EMB system in coal mine hoist, and achieve a approximately linear relationship between motor and positive pressure.

Currently, Electro-hydraulic-braking (EHB) system (one structure type of BBW systems) has become more and more popular and mature in automotive field, while EMB still stay on theoretical and experimental stage without reaching safety regulations. In view of this, some research achievements of mature EHB applications also can guide our research ideas for our reference. For dealing with the uncertainties and disturbances of EHB system, Shi and Huang et al.¹¹ proposed a dual-loop braking pressure control method with speed and current tracking controllers. In ¹², an adaptive sliding mode controller combining desired-state and integral-antiwindup compensation facilitate the improvement of the system steady tracking performance. To consider the significantly nonlinear behaviors of Integrated-braking-control (IBC) system which is an electro-mechanical-hydraulic coupling system and critical impact of vehicle dynamics on cylinder pressure estimation precision, ¹³ adopted EKF method to estimate cylinder pressure error based on hybrid of hydraulic model and single-wheel one whose error is always less than 2MPa in typical road. Also for dealing with actual friction problem, In ¹⁴, linearizing the nonlinear Tustin friction model improve pressure-tracking accuracy, a sliding mode controller is utilized to suppress friction disturbances, and subsequently Lyapunov method verified its stability.

The existing literature also indicates that response speed of EHB system may be slower than EMB because of pressure transfer delay in hydraulic pipelines. Especially when tackling with nonlinear problems of electro-mechanical-hydraulic couple and hydraulic pressure hysteresis characters as well as hydraulic parameters uncertainty disturbance caused by hydraulic leak and working temperature variation, braking force tracking performance seems to be obviously weaker than EMB. In fact, current braking system of UTRV is traditional hydraulic system manipulated by driver without close-loop and decoupled control performance, whose pressure response time is

significantly longer than EMB. Therefore, it is beneficial for improvement of braking safety and active control performance of underground auxiliary transportation system to research and develop a practical EMB system of UTRV with force close-loop feedback to track clamping force.

In generally, The main contributions of this paper are listed as follows:

- We develop a practical clamping force controller with cascade three-close-loop control architecture, which can also achieve adaptive tracking of clamping force & automation adjustment of gap distance. The clamping force response rate is obviously faster than traditional hydraulic braking method.
- we propose a contact point detection method to achieve control mode switch between gap distance control and clamping force control.
- Simulation and experiment verified above two contents.

The rest parts of this paper are described as follows. The next section introduces modeling and analysis of EMB. Section III presents the overall control system, involving of cascaded three-closed-loop control method with contact point detection technology utilized for force/position control mode switch. The results and analysis of simulations based on software model and experiments of prototype in real mine vehicle are shown in Section IV. Finally, Section V describes some conclusion.

2. Mathematical Modeling of EMB

The Electro-mechanical brake generates initial force by a surface-mounted permanent magnet synchronous motor (SPMSM) whose advantage involves high power density and small size. The reminder parts in this EMB also include a planetary reduction gear, a ball screw, a pair of frictional pads and a braking disk. It is seen in Figure 1 that driver pushes the pedal to provide a braking intensity signal for the ECU of this EMB. The ECU calculates braking force command according to target braking intensity. EMB controller will send Pulse Width Modulation (PWM) signal corresponding to reference braking force into three-phase power inverter. And then the inverter provide 3-phase sine wave input for EMB motor to rotate. Further, the reduction gear and ball screw achieve function of motion conversion and force enlarging where the head part in screw directly compress frictional pads onto disk to make vehicle to decelerate and stop. In this work, the electro and mechanical subsystem model is discussed, respectively.

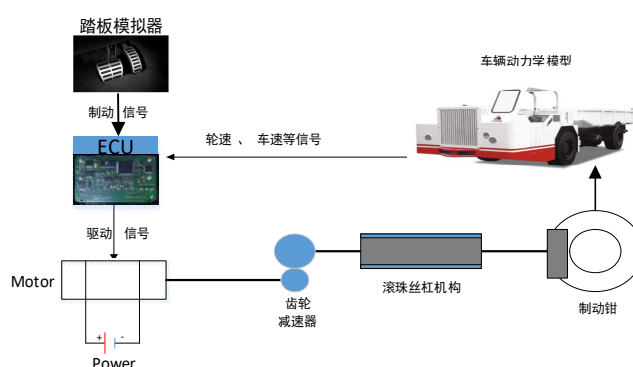


Figure 1. The schematic diagram of EMB for UTRVs.

2.1. Modeling of motor

2.1.1. PMSM model

Considering higher requirement towards speed and precision of braking force response, the surface permanent magnetic synchronous motor (SPMSM) is selected as torque motor in this EMB actuator [15]. We transformed current or voltage vectors in three-phase coordinates to stator orthogonal coordinates in two-phase $\alpha - \beta$ coordinates. And then, these vectors under $\alpha - \beta$ axis are transformed into the synchronous rotation d-q coordination. Coordinate transformation of above

two steps is expressed as follows 16 respectively, namely “Clarke transportation” and “Park transportation”.

$$\begin{bmatrix} f_\alpha \\ f_\beta \end{bmatrix} = \begin{bmatrix} 1 & -1/2 & -1/2 \\ 0 & \sqrt{3}/2 & -\sqrt{3}/2 \end{bmatrix} \begin{bmatrix} f_a \\ f_b \\ f_c \end{bmatrix} \quad (1)$$

$$\begin{bmatrix} f_d \\ f_q \end{bmatrix} = \begin{bmatrix} \cos\theta_e & \sin\theta_e \\ -\sin\theta_e & \cos\theta_e \end{bmatrix} \begin{bmatrix} f_\alpha \\ f_\beta \end{bmatrix} \quad (2)$$

where θ_e is the electrical rotor angle. Therefore, d-q voltage formula of PMSM are rewritten as follows:

$$\begin{cases} v_d = Ri_d + L_d \frac{di_d}{dt} - \omega_e \Psi_q \\ v_q = Ri_q + L_q \frac{di_q}{dt} + \omega_e \Psi_d \end{cases} \quad (3)$$

$$\begin{cases} \Psi_d = L_d i_d + \phi \\ \Psi_q = L_q i_q \end{cases} \quad (4)$$

where v_d, v_q is the d- and q-axis voltage; i_d, i_q is stator current in d-q axis; L_d, L_q are inductance in d-q coordinates; Ψ_d, Ψ_q is flux linkage in d-q coordinates and it can be expressed by $K_e = n_p \Psi_d$ where K_e presents back electromotive force constant and n_p presents pole pairs number; Relationship between electrical angle speed ω_e and mechanical angular speed ω_m can be expressed as $\omega_m \cdot \omega_e = n_p \omega_m / 2$; ϕ is flux linkage of rotor magnetic field; R presents stator resistance; The SPMSM torque equation can be show as equation (5)

$$T_m = \frac{3}{2} n_p [\phi i_q + (L_d - L_q) i_d i_q] \quad (5)$$

According to SPMSM principle, if i_d is fixed at zero, the torque will go up to maximum value 16. Hence, Equation (5) can further become a simple form similar to DC motor torque formula in which current can have a linear expression with torque:

$$T_m = \frac{3}{2} n_p \phi i_q \quad (6)$$

where a torque constant K_t further replace $\frac{3}{2} n_p \phi$. Therefore, the Eq. (6) can be simply again expressed as follows:

$$T_m = K_t i \quad (7)$$

2.1.2. Motor friction model

The motor of EMB is required to have a relatively high precision control performance, and the friction in the motor will directly affect the clamping force generated by the EMB system. Therefore, it is very important to establish an accurate motor friction model for improving the overall braking performance of the EMB system. In this paper, static friction characteristic models of static friction, Coulomb friction and viscous friction are selected. The static friction characteristic curve of the motor is shown in Figure 2, and the friction torque is given:

$$T_f = \begin{cases} T_m, & \dot{\theta} = 0, |T_m| < T_s \\ T_s \operatorname{sgn}(T_m), & \dot{\theta} = 0, |T_m| \geq T_s \\ T_c \operatorname{sgn}(\dot{\theta}) + B \dot{\theta}, & \dot{\theta} \neq 0 \end{cases} \quad (8)$$

where $\dot{\theta}$ is the relative sliding speed; T_m is the external torque, N·m; T_s is static friction moment, N·m; T_c is the coulomb friction torque, N·m.

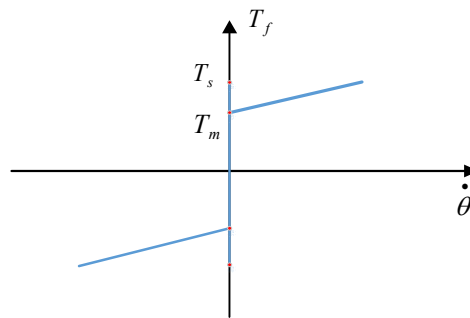


Figure 2. Static frictional characteristic curve of the motor.

2.2. Model of mechanical components

2.2.1. Mechanical transmission model

Reduction gear is utilized to enlarge force generated from motor. Subsequently, ball screw can generate linear motion of ball-screw nut which directly generates positive pressure on pad. Generally speaking, we can control position of screw nut via adjusting motor rotor angle displacement because they have a relatively linear mapping relationship between them¹⁸. The load torque T_L is generated from clamping force between pads and disk and can be calculated as follows:

$$T_L = \frac{1}{2\pi} \frac{L_s}{\eta_g n_g} \frac{1}{\eta_s} F_{cl} \quad (9)$$

where η_g presents efficiency coefficient of the gear box and η_s presents the one of ball screw; n_g is the reduction ratio of gear, L_s is lead of ball screw. Eq. (9) is usually expressed as $T_L = k_{cl} F_{cl}$ in which k_{cl} is total gearing transfer gain.

T_m should be specifically expressed as Eq.(10)

$$T_m = J_m \frac{d\omega_m}{dt} + B_f \omega_m + T_L \quad (10)$$

where J_m is rotor inertia constant and B_f is damping coefficient of the rotor .
where g is a actual nonlinear mapping principle of the θ_m .

2.2.2. Load model

The load torque of the motor comes from the thrust generated by the ball screw mechanism, and the brake liner generates a clamping force on the brake disc under the action of the thrust. There is a certain mathematical relationship between the clamping force of the EMB system and the shape variable of the friction disc [22], which indicates that the clamping force on the brake disc is given:

$$F_{cl} = A_1 s^3 + A_2 s^2 + A_3 s \quad (11)$$

where A_1, A_2, A_3 is the coefficient of the clamping force cubic polynomial; s is the shape variable of the friction plate, mm.

2.2.3. Brake Disc Model

The brake liner is installed in the caliper end, and the ball screw mechanism is used to push the brake disc to clamp, so that the left and right sides of the brake disc produce the same friction torque, which is given:

$$T_\mu = 2F_n \cdot R_b \cdot \mu_b \quad (12)$$

where F_n is the clamping force, N; μ_b is the friction coefficient of the friction plate; R_b is the effective radius of the brake disc, m.

Figure 3 presents our proposed EMB model in UTRVs. The voltage generated from three-phase inverter for motor operation is delivered to input ports of torque motor. The ball-screw θ_s and its displacement x_s have a proportional relationship expressed as $x_s = N_2 \theta_s$. $N_2 = L/2$, L is lead of ball screw. In this model, we also consider mapping relationship curve between x_s and F_{cl} as a cubic polynomial¹⁹ described as Eq.(11).

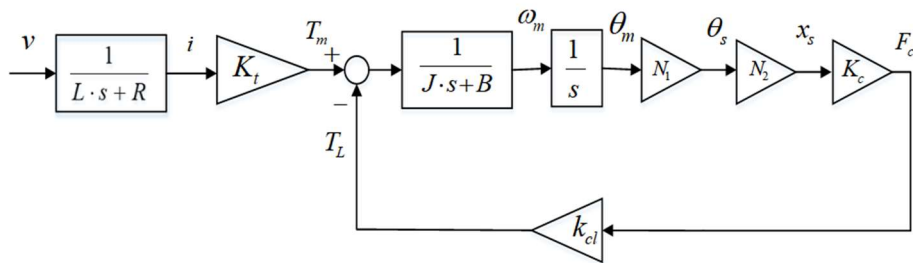


Figure 3. EMB system mathematical model.

3. Design of Controllers

3.1. Cascaded three close-loop Force/Position control strategies

Based on modeling of this EMB along with key contact point position detection technology introduced in Section II, a three-close-loop PI/PID control system for EMB in underground UTRVs is proposed because it's needed to be considered that very accurate EMB dynamic model in actual braking work condition is hard to be established, but tracking stability in steady-state of PID control method don't rely on detailed and precised mathematical model. The whose overall control architecture is shown in Figure 4.

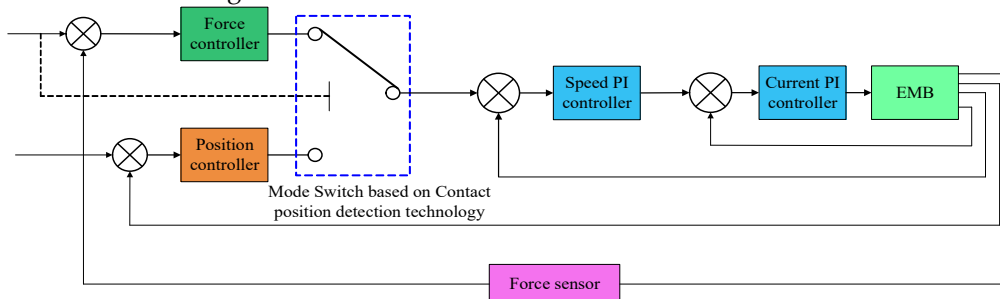


Figure 4. EMB control architecture.

It's can be seen in above model block diagram that the overall control system is cascaded architecture with three close-loop control units. Two Proportional-Integral (PI) feedback controllers with each different gain parameters is utilized for current and speed controllers of this EMB, respectively. However, both clamping force controller and contact point angle position

controller adopt PID method and provide target velocity of motor into subsequent speed control loop. The position controller aims to eliminate or reset the braking gap distance by utilizing relationship between the motor angular position θ_m and stoke displacement of screw nut x_s . After EMB local controller receive non zero measured value from load force sensor, The force controller start to work.

The comprehensive control of current, speed, and force close-loop units aims to make balance between transient response speed and steady-state tracking performance where data refresh rate of controlled variables in ECU is set around 20-50Hz.

3.1.1. Current loop

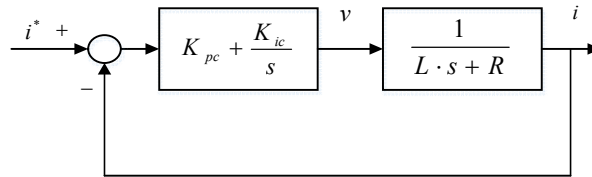


Figure 5. Current control loop.

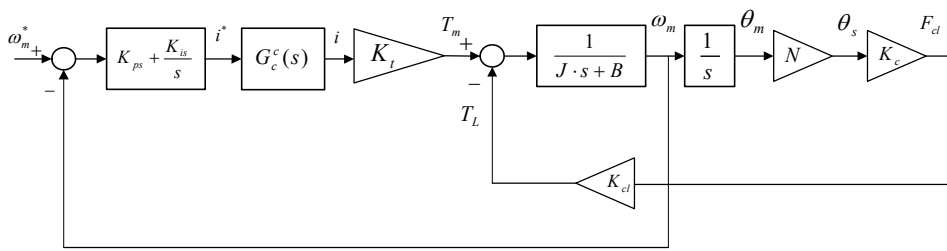
The current close loop PI controller is shown in Figure 6, Eq. (13) is its open loop transfer function.

$$G_c^o(s) = \frac{K_{pc}s + K_{ic}}{s} \frac{1}{Ls + R} = \frac{K_{pc} \left(s + \frac{K_{ic}}{K_{pc}} \right)}{Ls \left(s + \frac{R}{L} \right)} \quad (13)$$

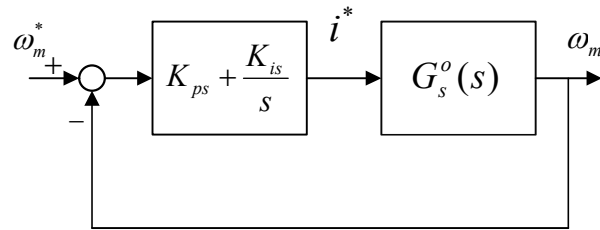
zero point of PI controller is designed to compensate for the pole of plant, such as in (14), the closed-loop transfer function can be written as (15). Proportional gain K_{pc} and integral gain K_{ic} are set to satisfy the given time-domain requirements on the current response.

$$\frac{K_{ic}}{K_{pc}} = \frac{R}{L} \quad (14)$$

$$\frac{I(s)}{I^*(s)} = G_c^c(s) = \frac{\frac{K_{pc}}{L}}{s + \frac{K_{pc}}{L}} \quad (15)$$



(a) Speed control loop with a detailed EMB model



(b) Speed controller with EMB transfer function

Figure 6. Speed control system.

3.1.2. Speed loop

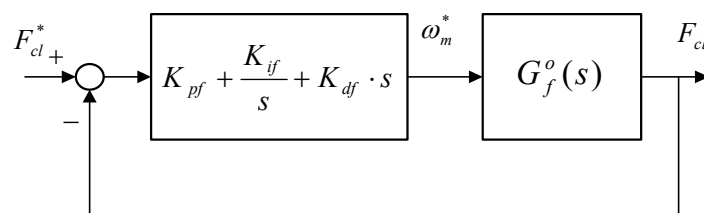
The motor speed controller is also a PI controller which is in front of current control loop in Figure 4. Detailed speed control loop model is in Figure 6(a).

The K_p and K_i of speed controller are obtained via pole placement method based on root locus and we have find the damping ratio and natural frequency meeting time- domain requirements of speed controller. In Figure 6(b), EMB transfer function $G_s^o(s)$ is calculated out and placed after the speed PI controller.

3.1.3 Force Controller

The actuator clamping force control is a PID controller which output reference speed. The clamping force control loop is shown in Figure 7 where the transfer function $G_f^o(s)$ is obtained as shown in Eq.(16). We also need to find the damping ratio and natural frequency corresponding to the desired pole locations based on requirements of force response in time-domain. The PID gains are obtained at dominant pole locations

$$G_f^o(s) = \frac{K_{ps} \cdot K_t \cdot K_{pc} \cdot N \cdot K_c / L \cdot s + K_{is} \cdot K_t \cdot K_{pc} \cdot N \cdot K_c / L}{J \cdot s^4 + (B + K_{pc} \cdot J / L) \cdot s^3 + (\cos \alpha \cdot r \cdot K_c \cdot N^2 + K_{pc} \cdot B / L + (K_{ps} \cdot K_t \cdot K_{pc} / L)) \cdot s^2 + ((K_{pc} / L) \cdot \cos \alpha \cdot r \cdot K_c \cdot N^2 + (K_{is} \cdot K_t \cdot K_{pc} / L)) \cdot s} \quad (16)$$

**Figure 7.** Clamping force close-loop control system

3.2. Estimation method of Contact Point utilized for Force/Position switch

It is necessary to estimate the critical contact position of pad and disk for transient switch process between force control mode and position control mode. Because motor of EMB always rotate related fixed revolutions after pads really contact the braking disk, we utilize rotor revolutions of torque motor to substitute angle position and control clamping force by tracking motor revolutions. We consider the relationship curve between the positive compressing force and motor rotor angle position as below form so that it is possible to control clamping force by motor angular position.

$$F_{cl} = g(\theta_m) \quad (17)$$

In this paper, motor revolutions corresponding to the contact point is achieved via experimental method. In Figure 8, the contact revolutions is 10.

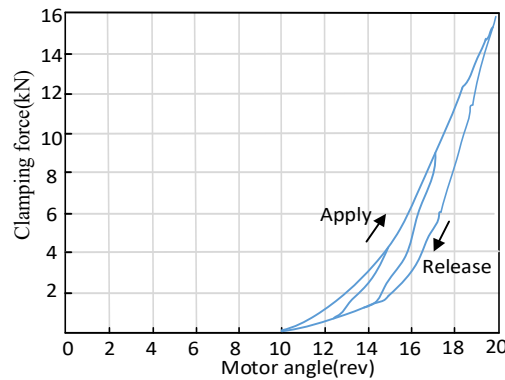


Figure 8. Clamping force test for contact point.

Aim at getting motor revolutions value which presents initial contact position of this EMB, we use a force sensor to provide feedback signal for motor angle position control of EMB. As actual force reaches command demand, the motor revolutions ranges from zero to 60. The measured signals for feedback include clamping force signal from pressure sensor ranging from 0-30kN, motor revolutions from encoder with precision of 360 count per turn and motor current signal from current sensor ranging from 0 to 30A.

4. Simulation results and discussion

The specific parameters of EMB apparatus used for both model simulation and development of prototype are listed in Table 1.

Table 1. The EMB system specific parameters.

Symbols	Physical meanings	Values
R	Motor resistance	10.2Ω
L_d, L_q	Motor inductance	0.075H
J_m	Rotor inertia	33.8gcm ²
B_m	Motor damping	0.21Ns/m
K_e	Back-emf constant	0.054V · s/rad
K_m	Motor torque constant	0.509Nm/A
n_p	Number of pole pairs	2
P_s	Pitch of ball screw	5mm
e_s	Efficiency of ball screw	92%
n_g	Total gear ratio	86:1
e_g	Efficiency of reduction gear	88%

The clamping force step response simulation in MATLAB/Simulink is shown in Figure 9. Dead-zone time is 45 ms. The raise time is 75 ms. The steady-state error is 118N(0.79%). After 190ms, system established stable clamping force at value of 15kN which is faster than traditional hydraulic braking.

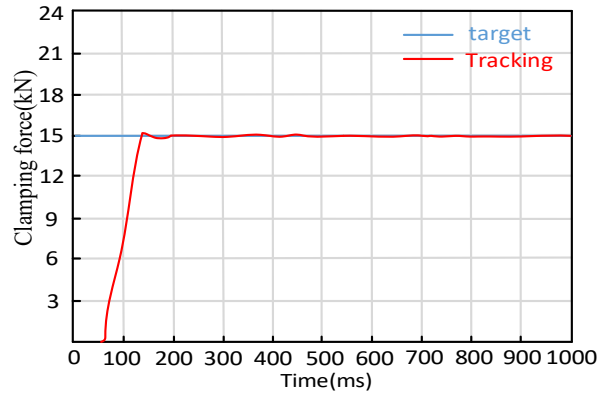


Figure 9. Clamping force step response of a three close-loop force control system.

5. Experimental Results and analysis

5.1. Experimental platform

In this work, it is seen in Figure 10 that we established an experimental EMB prototype controlled by our developed ECU with explosion-proof processing according to the safety standard of explosive atmospheres in underground coal mines. The metal terminals are the only electric signal transmission interface with inner electric parts in this white explosion-proof shell. The core of this ECU was an Infineon high performance micro-processor (32 bits) with many integrated interface circuits and meets the highest commercial vehicle safety level of D.



Figure 10. our developed ECU of intelligent chassis with explosion-proof processing.

System architecture of this prototype test in real rubber-tired vehicle is presented in Figure 11(a). We select a 400W (2.5N·m) surfaced PMSM supplied by a three-phase inverter power with DC input of 48V voltage as initial braking force source in this EMB system. Motor current measurement sensor ranges from 0-30A. The clamping force sensor ranges from 0-30kN. All of these signals simultaneously can feedback into the EMB local controller to achieve close-loop tracking control and also be collected into PC monitor software via high-speed data collector. The master controller of EMB managing the whole distributed braking system sends target braking force to the local controller (only one of four shown in Figure 11(a) as an example). The whole communication mode between every part in this prototype is Controller Area Network (CAN). The computer sends control signals to EMB controller which also can monitor experimental detailed operation process. The real vehicle test is conducted and implemented in test field of Keshi Group in Changzhou, China as shown in Figure 11(b).

Table 2 show the specific parameters used for simulation and experiment.

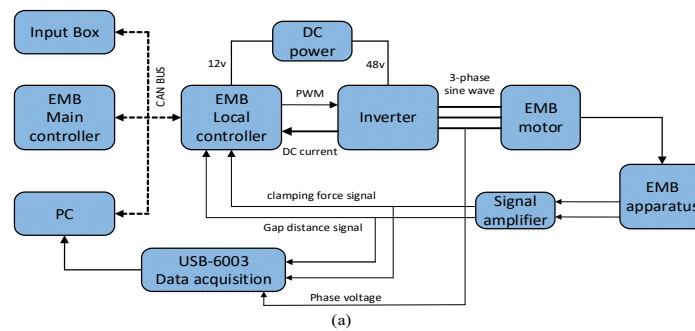


Figure 11. Experimental setup. (a) proposed EMB system block diagram; (b) test vehicle equipped with designed EMB.

5.2. Experimental Results

1. Brake clearance recovery test

Experimental initial state is that distance between friction pad and disk is zero mm. The target clearance is set to 1.5 ± 0.1 mm. When test is started, the braking command value is sent into local controller where the three-close-loop controller with proper gain parameter can fast tracking the input reference clearance value. within 500ms and keep stable.

It is shown in above Figure 12 that the initial 30ms is dead-zone of EMB and data receiver don't get any effective sensor data. After this time, braking motor began rotating. Rising time of braking clearance is 65ms. After 0.11s, Stead error range is 0.02mm. These indexes is obviously better than ones of traditional mechanical-hydraulic and electro-hydraulic braking method

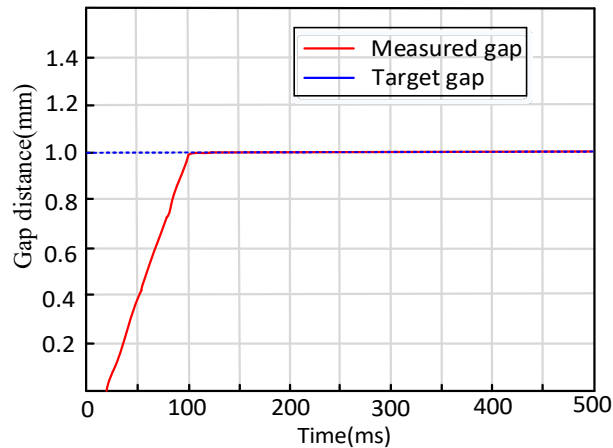


Figure 12. Brake clearance recovery experimental curve.

2. Brake positive pressure test

It is interesting to compare the braking clamping force step response curves between EMB system and traditional hydraulic pressure braking system as shown in Figure 14. According to total vehicle parameters calculation of underground UTRVs, the F_{nmax} related to EMB actuator performance is 60000N. Considering that the usual braking intensity of this vehicle is approximately 1/3, it's proper to set the step response test value of clamping force command at 20000N.

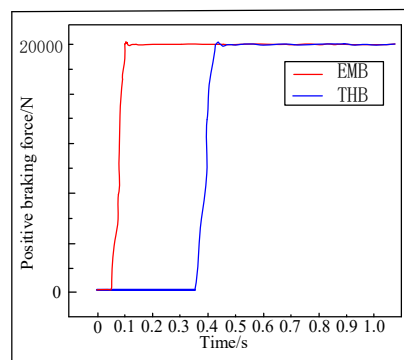


Figure 14. Positive pressure step response test curve.

The force response of EMB display that after dead-zone time(0.45s) caused by spending some time to eliminate gap and mechanical inertia, the control priority of the controller is received by force controller and the motor start to generate braking force. The system rise time is 0.125s which is sufficient to meet braking safety requirement based on National Coal Mine Safety Regulations. After 0.15s, the steady-state mean value of 19786N is reached at, the error is 186N(0.93%). The sum of dead-zone time and raise time of THB is .43s. It's obviously seen that proposed EMB system has more shorter braking acting time and shorter braking distance compared with THB, which means better vehicle safety.

6. Conclusions

In this paper, a novel EMB apparatus is proposed to replace the existing open-loop hydraulic brake which has intrinsic shortage such as slower response speed, lower automation level, hard maintenance and hydraulic oil leakage risk. Simulation and experimental curves present that this cascaded control strategy with three close-loop units can track target clamping force more rapidly and automatically adjust braking gap, which also can autonomously switch mode between force control mode and clearance distance control mode. This proposed EMB of mine electric trackless

rubber-tired can eliminate hydraulic climbing problem and shorten braking distance, which could have a significant enhancement on emergency braking safety of ETRV in coal intelligent transportation system.

Author Contributions: Conceptualization, J.L.; methodology, J.L.; software, J.L.; validation, J.L., Z.L.; formal analysis, J.L.; investigation, C.M.; resources, C.M.; data curation, J.L.; writing—original draft preparation, J.L.; writing—review and editing, Z.L.; visualization, J.L.; supervision, C.M.; project administration, C.M.; funding acquisition, X.X.; All authors have read and agreed to the published version of the manuscript.

Funding: This work was also supported by National Natural Science Foundation of China [grant numbers: 51975569, 51675520].

Data Availability Statement: The data that support the findings of this study are available from the corresponding author upon reasonable request.

Acknowledgments: The author(s) would like to express appreciations to Meilin Wang, Fahui Shi and other colleagues in Changzhou Keshi Group for their valuable support in the tests of real mine vehicle.

Conflicts of Interest: The authors declare no conflict of interest.

References

1. Song, Y.; Wang, N. Exploring temporal and spatial evolution of global coal supply-demand and flow structure. *Energy*. 2019, 168, 1073–1080.
2. Li, J.; Meng, G.; Xie, G., et al. Study on health assessment method of a braking system of a mine hoist. *Sensors*. 2019, 19, 769.
3. Zhang, Y.; Xu, G.; Zhang, X., et al. Design and research of the disc brake of mine hoists for monitoring the disc spring force and positive brake pressure. *Meas Sci Technol*. 2019, 30, 125903.
4. Jing, Houhua; Feng, Ruixue; Lin, Qinggan. Design and Test of Electro-Mechanical Brake Experiment System. *Proceedings of the 2022 6th CAA International Conference on Vehicular Control and Intelligence 2022*.
5. He, Cheng *, Hao, Chen †, Zhou, Yang *, and Weilong, Huang *. Braking Torque Closed-Loop Control of Switched Reluctance Machines for Electric Vehicles. *Journal of Power Electronics* 2015, 15, 469–478.
6. Fei, Xiao, Xiaoxiang, Gong, Zhihang, Lu, Lixia, Qian, Yiwei, Zhang, and Lifeng, Wang. Design and Control of New Brake-by-Wire Actuator for Vehicle Based on Linear Motor and Lever Mechanism. *IEEE Access* 2021, 9, 95832–95842.
7. Soohyeon, Kwon¹, Seonghun, Lee¹, Jaeseong, Lee¹. Daehyun, Kum¹. Accurate State Estimation for Electro-Mechanical Brake Systems. *Journal of Electrical Engineering & Technology* 2019, 14, 889–896.
8. Yiyun, Zhao, Hui, Lin, and Bingqiang, Li. Sliding-Mode Clamping Force Control of Electromechanical Brake System Based on Enhanced Reaching Law. *IEEE Access* 2021, 9, 19506–19515.
9. Chihoon, Jo, Sungho, Hwang, and Hyunsoo, Kim. Clamping-Force Control for Electromechanical Brake. *IEEE Transactions on Vehicular Technology* 2010, 59, 3205–3212.
10. Huawei, Jin; Huawei, Xu; Shun, Wang. Design and test of electromechanical disc brake controller for mine hoist. *Measurement and Control* 2022, 55, 146–148.
11. Jialei, Shi, Chao, Huang, Xiangyu, Wang, Liang, Li. Adaptive Dual-Loop Hydraulic Pressure Controller for Electric Booster Brake System. *IEEE 28th International Symposium on Industrial Electronics* 2019, 1481–1486.
12. Lu, Xiong, Wei, Han, Zhuoping, Yu. Adaptive sliding mode pressure control for an electro-hydraulic brake system via desired-state and integral-antiwindup compensation. *Mechatronics* 2020.
13. Haichao, Liu, Lingtao, Wei, Hongqi, Liu, Jinjun, Wu, and Liang, Li. Brake Pressure Estimation of the Integrated Braking System Considering Vehicle Dynamics. *Actuators* 2022, 1–15.
14. Jiawang, Yong, Feng, Gao, Nenggen, Ding, Yuping, He. Pressure-tracking control of a novel electro-hydraulic braking system considering friction compensation. *Journal of Center South University* 2017, 24, 1909–1921.
15. C.-Y. Lin and Y.-C. Liu. Precision tracking control and constraint handling of mechatronic servo systems using model predictive control. *IEEE/ASME Trans. Mechatronics*. 2012, 17, 593–605.
16. Beak, SK, Oh, HK, Kwak, MH, et al. A design method of three phase IPMSM and clamping force control of EMB for high-speed train. *J Korea Academia-Industrial Cooperation Soc.* 2018, 19, 578–585.
17. Weng, J, Tian, C, Wu, M, et al. Coupled rigid-flexible modelling and dynamic characteristic analysis of electromechanical brake (EMB) units on trains. *Proc Inst Mech Eng F J Rail Rapid Transit*. 2020, 235, 700–712.
18. Jo, C, Hwang, S, Kim, H. Clamping-force control for electromechanical brake. *IEEE Trans Veh Technol*. 2010, 59, 3205–3212.

19. Qiping Chen, Zongyu Lv, Haiyang Tong and Zuqi Xiong. Clamping Force Control Strategy of Electro-Mechanical Brake System Using VUF-PID Controller. *Actuators* 2023;12,272:3-4.
20. Park Giseo, Choi Seibum, Hyun Dongyoon. Clamping force estimation based on hysteresis modeling for electro-mechanical brakes. *Int J Automot Technol.* 2017,18,883–890.
21. Yijun Li, Taehyun Shim, Dong-Hwan Shin, Seonghun Lee, and Sungho Jin. Control System Design for Electromechanical Brake System Using Novel Clamping Force Model and Estimator. *IEEE Transactions on Vehicular Technology* 2021;70(9):8653-8668.
22. Liu, Z.; Chen, Y.; Chen, L. A Gap Control Method for Electromechanical Brakes. *Acta Armamentarii* 2022, 43, 1478–1487.

Disclaimer/Publisher's Note: The statements, opinions and data contained in all publications are solely those of the individual author(s) and contributor(s) and not of MDPI and/or the editor(s). MDPI and/or the editor(s) disclaim responsibility for any injury to people or property resulting from any ideas, methods, instructions or products referred to in the content.